1575

Reprinted from

QUATERNARY SCIENCE REVIEWS

Vol. 19, No. 1–5, pp. 285–299

Study of abrupt climate change by a coupled ocean-atmosphere model

SYUKURO MANABE and RONALD J. STOUFFER

Institute for Global Change, 7F SEAVANS N Bldge., Shibaura 1-2-1 Minatota-ku, Tokyo 105 6791, Japan
Geophysical Fluid Dynamics Laboratory/NOAA, Princeton University, Princeton NJ 0854, USA

This paper is rewritten for the recent PAGES Open Science meeting, revising the paper published earlier in *Paleoceanography* (12 (1997), 321-336). It contains the improved discussion of the suggested mechanism for abrupt climate change.

PERGAMON

Quaternary Science Reviews 19 (2000) 285–299

QSR

Study of abrupt climate change by a coupled ocean–atmosphere model

Syukuro Manabe[a,*], Ronald J. Stouffer[b]

[a]*Institute for Global Change Research, Frontier Research System for Global Change, 7F SEAVANS-N Bldg. Shibaura 1-2-1, Minato-ku, Tokyo 105-6791, Japan*

[b]*Geophysical Fluid Dynamics Laboratory/NOAA, Princeton University, Princeton, NJ 08542, USA*

Abstract

This study examines the responses of the simulated modern climate of a coupled ocean–atmosphere model to the discharge of freshwater into the North Atlantic Ocean. Two numerical experiments were conducted. In the first numerical experiment in which freshwater is discharged into high North Atlantic latitudes over the period of 500 years, the thermohaline circulation (THC) in the Atlantic Ocean weakens. This weakening reduces surface air temperature over the northern North Atlantic Ocean and Greenland and, to a lesser degree, over the Arctic Ocean, the Scandinavian peninsula, and the Circumpolar Ocean and the Antarctic Continent of the Southern Hemisphere. Upon termination of the water discharge at the 500th year, the THC begins to reintensify, gaining its original intensity in a few hundred years. As a result, the climate of the northern North Atlantic and surrounding regions resumes its original distribution. However, in the Pacific sector of the Circumpolar Ocean of the Southern Hemisphere, the initial cooling and recovery of surface air temperature is delayed by a few hundred years. In addition, the sudden onset and the termination of the discharge of freshwater induces a multidecadal variation in the intensities of the THC and convective activities, which generate large multidecadal fluctuations of both sea surface temperature and salinity in the northern North Atlantic. Such oscillation yields almost abrupt changes of climate with rapid rise and fall of surface temperature in a few decades. In the second experiment, in which the same amount of freshwater is discharged into the subtropical North Atlantic over the period of 500 years, the THC and climate evolve in a manner qualitatively similar to the first experiment. However, the magnitude of the THC response is 4–5 times smaller. It appears that freshwater is much less effective in weakening the THC if it is discharged outside high North Atlantic latitudes. The results from numerical experiments conducted earlier indicate that the intensity of the THC could also weaken in response to a future increase of atmospheric CO_2, thereby moderating the CO_2-induced warming over the northern North Atlantic and surrounding regions. Published by Elsevier Science Ltd.

1. Introduction

Isotopic analysis of Greenland ice cores (e.g., Grootes et al., 1993) suggests that large and rapid changes of climate occurred frequently during the last glacial and deglacial periods. For example, the isotopic ($\delta^{18}O$) temperature dropped very rapidly approximately 13,000 years ago, followed by the so-called Younger Dryas event (Y-D) when the isotopic temperature was almost as low as at the last glacial maximum. Faunal and palynological analyses indicate that during the cold Y-D period, surface temperatures were very low not only over the northern North Atlantic but also over Western Europe. The Y-D period lasted several hundred years and ended abruptly, as indicated by the records from Greenland ice cores. Broecker et al. (1985) suggested that such an abrupt change resulted from a very rapid change in the thermohaline circulation (THC) from one mode of operation to another. They further speculated that meltwater from continental ice sheets caused the capping of the oceanic surface by relatively freshwater in high North Atlantic latitudes and was responsible for the rapid weakening of THC and the abrupt cooling of climate.

This essay explores the physical mechanism of abrupt climate change based upon the results from a set of numerical experiments conducted at the Geophysical Fluid Dynamics Laboratory of NOAA. Particularly, it attempts to elucidate the role of the thermohaline circulation (THC) in inducing the abrupt climate change.

* Corresponding author.

E-mail addresses: sm@frontier.esto.or.jp (S. Manabe), rjs@gfdl.gov (R.J. Stouffer)

0277-3791/99/$ - see front matter Published by Elsevier Science Ltd.
PII: S0277-3791(99)00066-9

Broecker et al. (1988) speculated that the diversion of meltwater from the Mississippi to the St. Lawrence River was responsible for reducing the rate of deep-water formation during the Y-D. Although convincing evidence for this meltwater diversion at the beginning of the Y-D has not been found, it is likely that meltwater is the most effective in reducing the deep-water formation when it is discharged near the sinking region of the THC. In order to evaluate the effectiveness of a high-latitude versus low-latitude discharge onto the North Atlantic for weakening of the THC, we conducted two numerical experiments. In the first experiment, freshwater is discharged onto high latitude North Atlantic Ocean, whereas in the second experiment it is discharged onto the subtropical latitudes.

This paper is a modified and shortened version of a recent paper by Manabe and Stouffer (1997), hereafter identified as MS97, for presentation at the IGBP PAGES First Open Science Meeting. It incorporates some of the perspectives which have been acquired since the publication of the paper. In the final section, it discusses the possibility of future change in the THC based upon the results of numerical experiments recently conducted at the Geophysical Fluid Dynamics Laboratory of NOAA.

2. Coupled model

2.1. Model structure

The coupled atmosphere–ocean–land surface model used here was developed to study the climate response to increasing greenhouse gases, and will hereafter be called the coupled model, for simplicity. The structure and performance of the model were described by Manabe et al. (1991), hereafter identified as M91. Therefore, only a brief description of the model structure is given here.

The coupled model (Fig. 1) consists of general circulation models (GCM) of the atmosphere and ocean, and a simple model of the continental surface that involves the budgets of heat and water (Manabe, 1969). It is a global model with realistic geography limited by its resolution. It has nine vertical finite difference levels. The horizontal distributions of predicted variables are represented by spherical harmonics (15 associated Legendre functions for each of 15 Fourier components) and by gridpoint values (Gordon and Stern, 1982). The model uses a simple scheme of land-surface process to compute surface fluxes of heat and water. Insolation varies seasonally, but not diurnally. The model predicts cloud cover which depends only on relative humidity.

The ocean GCM (Bryan and Lewis, 1979) uses a full finite-difference technique and has a regular grid system with approximately 4° latitude by 3.7° longitude spacing. There are 12 vertical finite-difference levels. The atmospheric and oceanic components of the model interact with each other once each day through the exchange of heat, water, and momentum fluxes. A simple sea ice model is also incorporated into the coupled model. It predicts sea ice thickness, based upon thermodynamic heat balance and incorporating the effect of ice advection by ocean currents. For further details of the coupled model, see M91. Dixon et al. (1996) also describe the

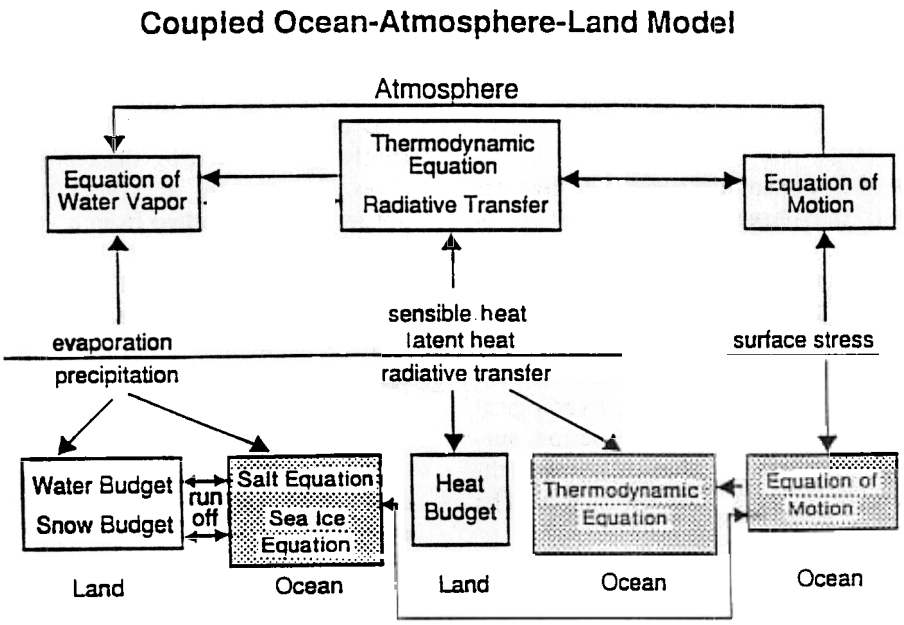

Fig. 1. The structure of the coupled ocean–atmosphere model.

ability of the model to simulate the uptake of anthropogenic chlorofluromethane (CFC-11) by the ocean.

2.2. Time integration

Initial conditions for the time integration of the coupled model include realistic seasonal and geographical distributions of surface temperature, surface salinity, and sea ice of the present with which both the atmospheric and oceanic model states are nearly in equilibrium. When the time integration of the model starts from this initial condition, the model climate drifts toward its own equilibrium state, which differs from the initial condition described above. To reduce this drift, the fluxes of heat and water imposed at the oceanic surface (including sea ice-covered areas) of the coupled model are modified by amounts that vary geographically and seasonally but do not change from one year to the next (for details, see M91 and Manabe and Stouffer, 1994). Since the adjustments are determined prior to the time integration of the coupled model and are not correlated to the anomalies of SST (i.e., sea surface temperature) and SSS (i.e., sea surface salinity), which can develop during the integration, they are unlikely to either systematically amplify or damp the anomalies. Owing to the flux adjustment technique, the model fluctuates around a realistic equilibrium state.

Starting from the initial condition that was obtained and described above, the coupled model is integrated over a period of 1000 years. Owing to the application of the flux adjustments, the mean trend in global mean surface air temperature during this period is only $-0.023°C\ century^{-1}$. The trend of global mean temperature in the deeper layers of the model ocean is somewhat larger at $-0.07°C\ century^{-1}$. This trend appears to result from the imperfection of the procedures used for determining the initial condition and time integration of the coupled model. The specific reasons for this trend, however, have not been identified and are under investigation.

3. Design of freshwater experiments

The simulated modern state of the coupled ocean–atmosphere system, which is obtained from the time integration described in Section 2.2 is used as the control for the freshwater experiments conducted in the present study. Instead, one could have used as a control a coupled model state of the last deglaciation period when a major fraction of the continental ice sheets of the last glacial period still remained. Since the response of the cold, glacial state of the coupled ocean–atmosphere system to freshwater discharge could be different from the corresponding response of the interglacial, modern state (e.g. Winton, 1997), it is highly desirable to conduct the numerical experiments using boundary conditions of the last deglaciation period. However, we have not succeeded in simulating either the glacial or deglacial world satisfactorily using a coupled ocean–atmosphere GCM. Thus, we cannot help using the simulated modern state of the coupled model as a control and perturbed it with an input of freshwater into the North Atlantic Ocean.

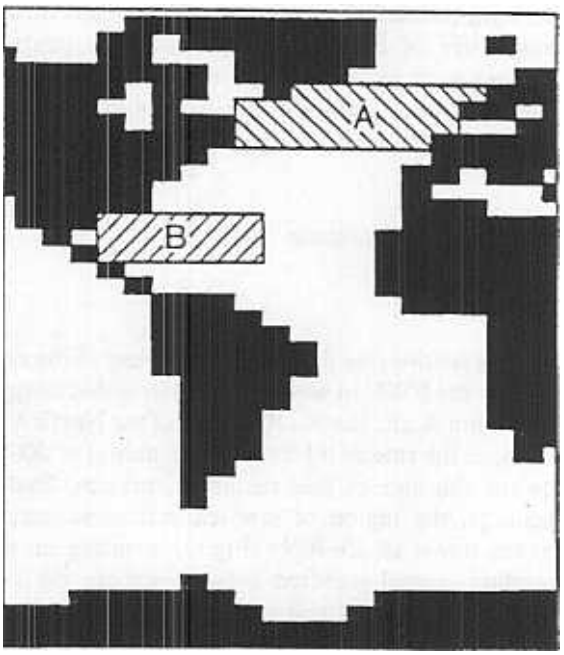

Fig. 2. Regions A and B indicate the areas where freshwater is discharged in the first freshwater integration (FWN) and the second freshwater integration (FWS), respectively (from MS97).

In addition to the control integration described in Section 2.2, two numerical integrations are conducted for the present study. The initial condition for both integrations is the state of the coupled model at the 500th year of the control integration. In the first freshwater integration (FWN), the freshwater is discharged at the rate of 0.1 Sv (one sverdrup $= 10^6\ m^3\ s^{-1}$) uniformly over the 50–70°N belt of the North Atlantic Ocean (identified as domain A in Fig. 2) over the period of 500 years. After the termination of the freshwater discharge, the FWN is continued for the additional 750 years until the 1250th year. By comparing the FWN with the control integration over the corresponding period of 1250 years, the impact of freshwater input upon the coupled ocean–atmosphere model is investigated.

In the second freshwater integration (FWS), freshwater is discharged uniformly over the subtropical region, identified as domain B (20.25–29.25°N, 52.5°–90.0°W) in Fig. 2, again at the rate of 0.1 Sv over the period of 500 years. This integration is completed at the 750th year (i.e., 250 years after the termination of the freshwater discharge).

In both numerical experiments, it is assumed that the temperature of discharged freshwater is identical to the local surface temperature of the ocean. Thus, the freshwater input changes only surface salinity without affecting surface temperature.

4. Freshwater experiment

4.1. FWN

In this section, we discuss the response of the coupled model in the FWN in which freshwater is discharged into the domain A, i.e., the 50–70°N belt of the North Atlantic Ocean, at the rate of 0.1 Sv over the period of 500 years. Toward the end of this sustained, massive freshwater discharge, the region of low sea surface salinity (SSS) spreads down to 30–40°N (Fig. 3), creating an intense halocline several hundred meters beneath the surface. The surface layer of relatively fresh, low-density water prevents the convective cooling of the water column and the production of negative buoyancy in the sinking region of the thermohaline circulation (THC) in the northern North Atlantic, thereby weakening the THC during the 500-year period of the freshwater discharge. The streamfunction of the meridional overturning in the Atlantic Ocean (Fig. 4) indicates that the THC not only weakens but also becomes much shallower (Fig. 4b). Meanwhile, the northward flow of Antarctic bottom water extends northward, intensifying the reverse overturning cell near the bottom of the Atlantic Ocean (Fig. 4b). Following the termination of freshwater discharge on the 500th year, the THC reintensifies and fully recovers its original intensity and distribution by the 900th year (Fig. 4c).

As the intensity of the THC weakens, the surface currents in the North Atlantic Ocean also undergo marked changes, which can be inferred by comparing Fig. 5a and b. For example, the North Atlantic Current, which extends from the Florida coast towards the Norwegian Sea, also weakens in the Atlantic throughout the period of the freshwater discharge. Thus, the warm, saline surface water in the subtropical Atlantic hardly penetrates into the northern North Atlantic Ocean towards the end of the 500-year period of freshwater discharge. On the other hand, the Subarctic Gyre and associated East Greenland Current become more intense and extend southwards. It is of particular interest that the intensified Labrador Current and its southeastward extension track the path of ice-rafted debris during the so-called Heinrich events (Bond et al., 1992), which appear to resemble the Y-D event in many respects.

Associated with the weakening of the THC described above, the northward advection of the warm and saline surface water is reduced, causing a large reduction in sea surface temperature (SST) in the northern North Atlantic (Fig. 6). The local maximum in cooling located south of Greenland, however, is attributable to the intensification and the southward extension of the east Greenland Current (Fig. 5) which advects cold Arctic surface water southward.

Interestingly, an extensive region of SST reduction appears not only in the North Atlantic but also in the Circumpolar Ocean of the Southern Hemisphere. The cold anomalies in the Atlantic/Indian Ocean sector change approximately in phase with the cold anomalies in the North Atlantic and begin to weaken after the termination of the freshwater discharge. However, the cold anomalies in the Pacific sector of the Circumpolar Ocean continue to intensify until ~ 300 years after the

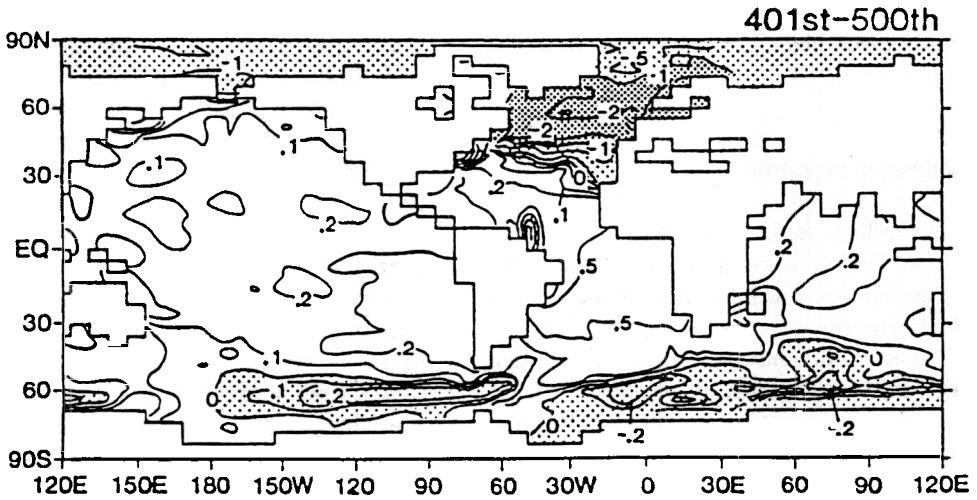

Fig. 3. The geographical distribution of SSS anomalies (psu) averaged over years 401–500 of the FWN. The anomalies represent the difference between the FWN and the control experiment. Contours are in logarithmic intervals for values of 0, ± 0.1, ± 0.2, ± 0.5, ± 1 and ± 2 (from MS97). The regions of negative anomaly are shaded.

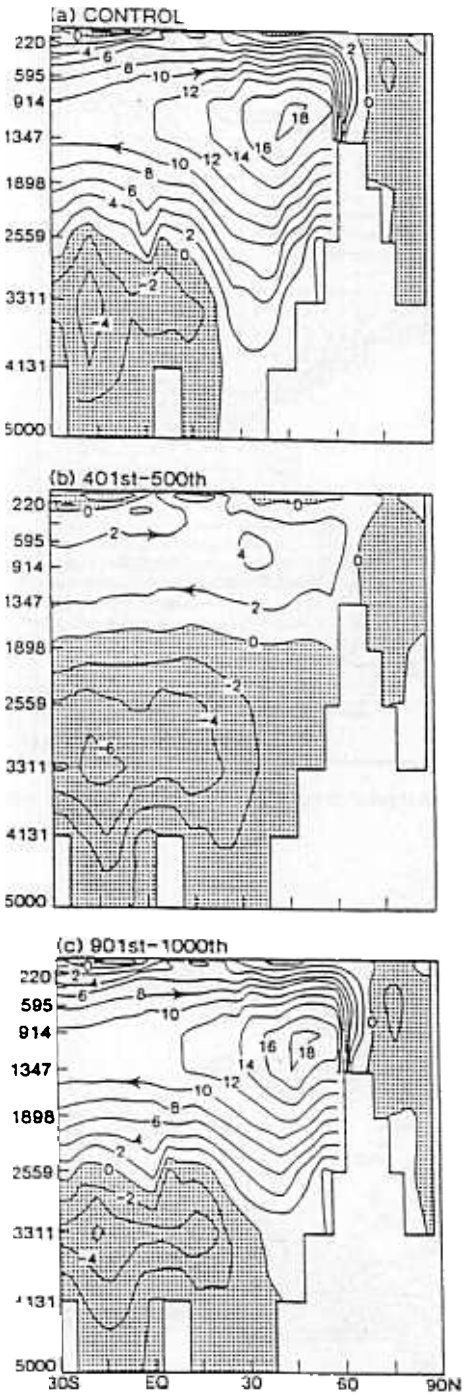

Fig. 4. Streamfunction of the THC in the Atlantic Ocean of the coupled model in units of sverdrups. (a) Control experiment (100-year average taken just prior to starting the FWN). (b) Average over years 401–500 of the FWN. (c) Average over years 901-1000 of the FWN. On the left-hand side of each panel, depth is indicated in meters (from MS97).

termination. Preliminary analysis indicates that this anomaly results from the delayed weakening of the deep reverse THC cell involving the Antarctic Bottom Water in the Pacific Ocean. The weakening increases the meridional SST gradient of the Circumpolar Ocean and intensifies the surface westerlies which, in turn, reduces SST by enhancing the northward Ekman drift of cold surface water and sea ice and further increases the meridional SST gradient (MS97).

The freshwater-induced change of sea surface temperature described above affects the overlying atmosphere, causing a reduction in surface air temperature over extensive region (Fig. 7). The cooling is particularly large over the northern North Atlantic and the Nordic Seas, and extends over not only Greenland but also the Arctic Ocean, the Scandinavian Peninsula, and Western Europe (Fig. 7). Also, small negative anomalies extend over most of the high northern latitudes. The cooling centered around Iceland increases until the end of the freshwater discharge (i.e., the 500th year of the experiment), but decreases rapidly thereafter and disappears completely by the 750th year. Negative anomalies also appear in the Indian and Pacific sectors of the Circumpolar Ocean of the Southern Hemisphere, extending to the Antarctic Continent. On the other hand, very small positive SST anomalies cover the rest of the world. The global mean change of surface air temperature are small throughout the course of the experiment because small but extensive positive temperature anomalies compensate for the large but geographically limited negative anomalies.

The distribution of the freshwater-induced change in surface air temperature described above is consistent with the signitures of significant Y-D cooling, which was prepared by D. Peteet (Broecker, 1995) based upon the analysis of oceanic and bog sediments (Fig. 8). Over the Western Europe and Labrador Peninsula, for example, polynological records indicate the Y-D cooling of significant magnitude, whereas they do not over most of North American Continent. The qualitative resemblance between the two patterns encourages the speculation that the cold climate of the Y-D could have resulted from the slow-down of the THC which was induced by an input of freshwater, such as the discharge of the meltwater from the continental ice sheets. The pattern of the model-generated change, however, does not extend sufficiently toward low latitudes compared to the pattern of the Y-D/Alleröd difference determined from proxy data. As discussed in Section 6, this discrepancy may be partly attributable to the fact that the freshwater flux is applied to the simulated, modern state of the coupled ocean–atmosphere model which is much warmer than the cold state of the deglacial period. Thus, the albedo feedback process involving sea ice and snow operates at higher latitudes, confining the freshwater-induced temperature change poleward of the regions of the Y-D cooling.

The model atmosphere is not a passive participant in the simulated cooling event. Associated with the cooling, a positive sea level pressure anomaly (max. ~ 4 mb) with a meridionally elongated pattern develops around

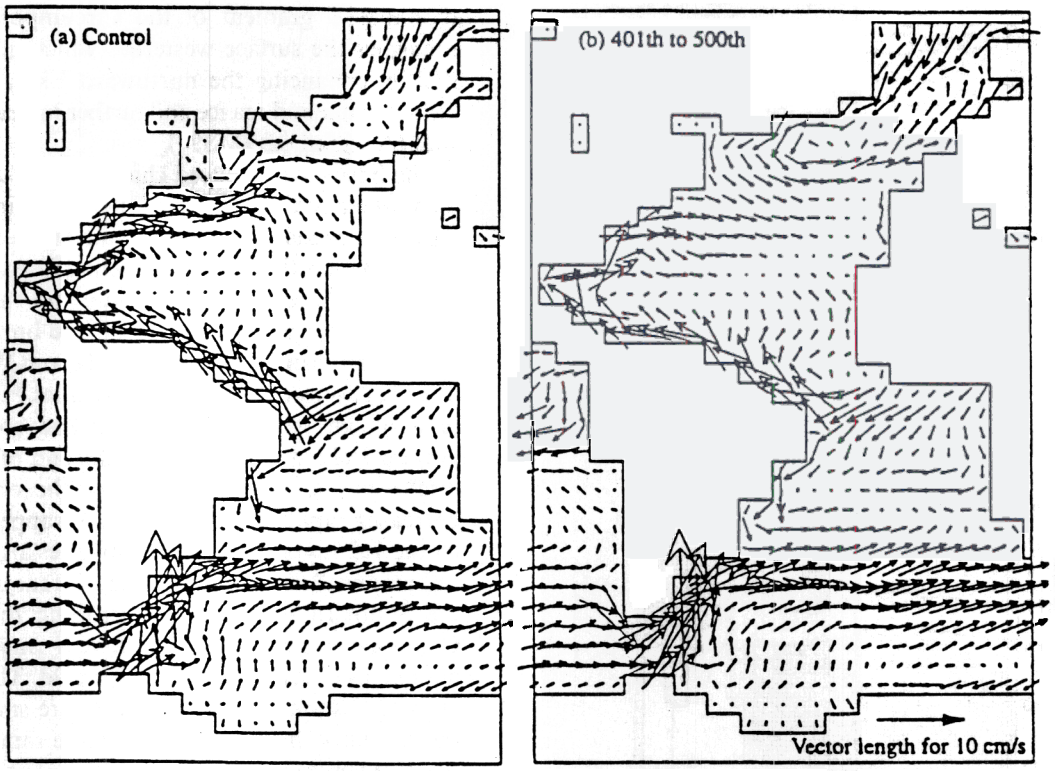

Fig. 5. Map of surface current vectors. (a) Control experiment (100 year average taken just prior to starting the FWN). (b) Average over year 401–500 of the FWN (from MS97).

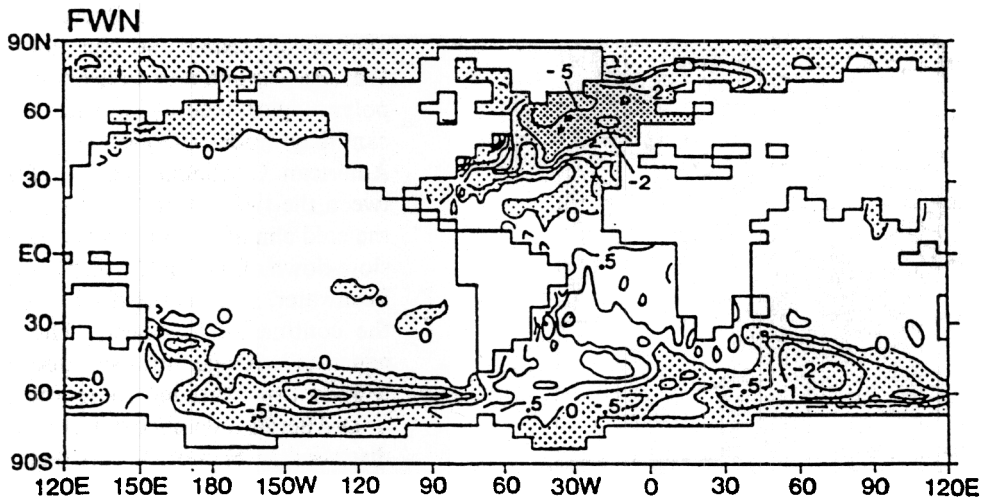

Fig. 6. Geographical distribution of SST anomalies (°C) averaged over year 401–500 of the FWN. The anomalies are defined as the difference between the FWN and the control experiment (from MS97).

southeastern Greenland (Fig. 9), resulting in the weakening and slight eastward shift of the Icelandic Low and a marked weakening of southerly wind over the Greenland Sea. Thus, the East Greenland Current intensifies along the east coast of Greenland and extends southward and reduces SSS around Iceland, thereby contributing to the weakening of the THC. On the other hand, Marotzke (1990) noted that the weakening of the Icelandic Low leads to a reduction in the intensity of the westerlies, and accordingly, that of equatorward Ekmann drift currents which could contribute to the reintensification of the THC. In the present experiment, however, the positive

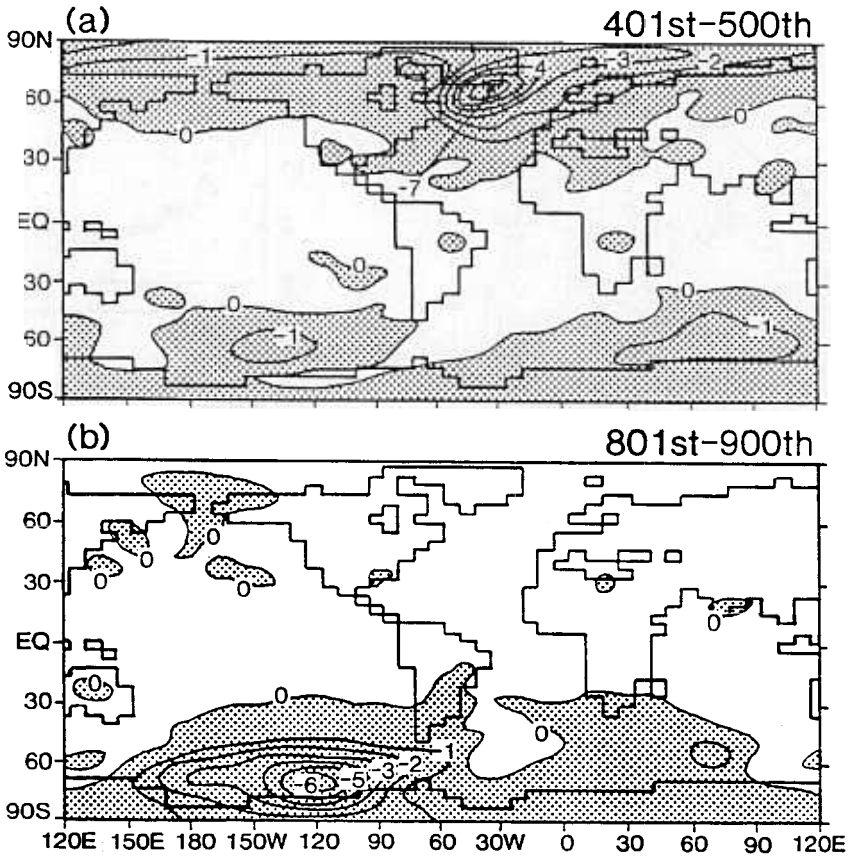

Fig. 7. The geographical distributions of surface air temperature anomalies (°C) averaged over (b) years 401–500 and (d) years 801–900 of the FWN. The anomalies represent the difference between the FWN and the control experiment (from MS97).

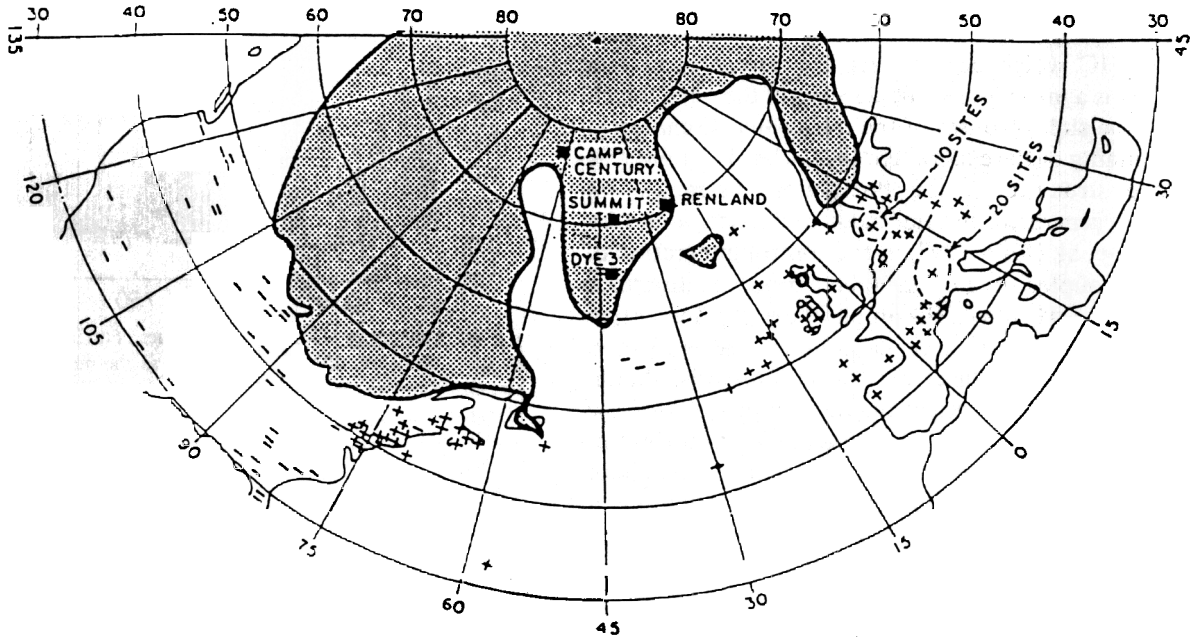

Fig. 8. Map prepared by D. Peteet showing sites of ocean sediment (planktonic forams) and bog sediments (pollen grains) where records covering the interval of deglaciation are available. The pluses (minuses) indicate that the Younger Dryas event (Y-D) cooling is seen (not seen). Two pluses are added by the present authors at 43.5°N, 29.9°W and 33.7°N, 57.6°W, referring to the studies of Keigwin and Lehman (1994), and Keigwin and Jones (1989), respectively. The locations of the Greenland ice cores (all show the Y-D) are also given. The shaded region shows the area coverage of the ice cap at the time of the Y-D (from Broecker, 1995). See also Fig. 6 of Peteet (1995) which indicates the global distribution of polynological evidence for the Y-D cooling.

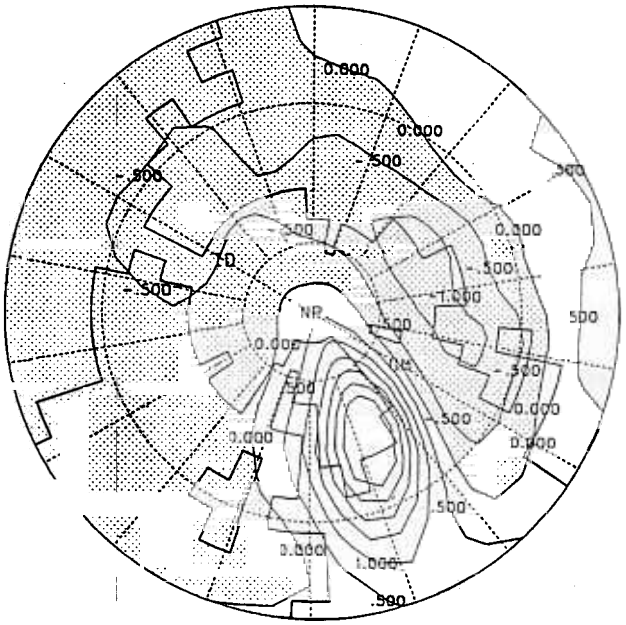

Fig. 9. Geographical distribution of annual mean anomalies of sea level pressure (mb) averaged over years 401–500 of the FWN. The anomalies are defined as the difference between the FWN and the control experiment. The upper and lower vetical lines (dotted) in the middle of the figure indicate 120° E and 60° E longitudes, respectively.

sea level pressure anomaly does not extend westward far enough to reintensify the THC. Instead, it appears to contribute to further weakening of the THC as noted above.

Superimposed upon the weakening and intensification of the THC which occurs over the period of several centuries, is a multidecadal fluctuation of the THC which follows the sudden onset of the freshwater discharge at the beginning of the experiment (Fig. 10a). The timescale and the structure of the fluctuation resembles the internally generated, multidecadal oscillation found by Delworth et al. (1993, 1997) in the control integration of the same coupled ocean-atmosphere model as described in Section 2.2. However, the amplitude of the fluctuation is much larger than that of the multidecadal oscillation identified by Delworth et al. The multidecadal fluctuation of the THC is approximately in-phase with the corresponding fluctuations of SSS and SST. Shortly after the start of the water discharge, a very rapid drop of both SSS and SST occurs, followed by large oscillations of both variables with a timescale ranging from several decades to a century (Fig. 10b and c). The amplitudes of the oscillations gradually decrease until the termination of freshwater discharge (i.e., the 500th year) due to the growth of sea ice, which reduces the anomalies of both SST and SSS through melting and freezing. The amplitude, however, increases again a few hundred years later, generating repeated, almost abrupt warming and cooling with decadal time scale (Fig. 10b).

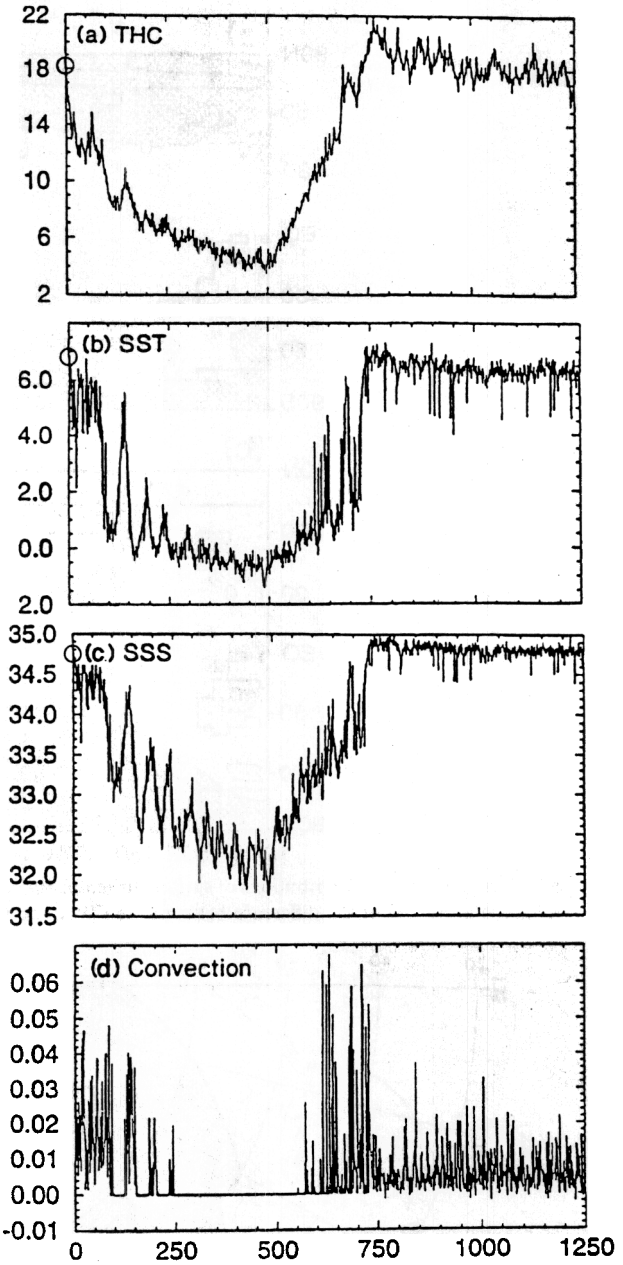

Fig. 10. Time series of annual mean values of (a) intensity of the THC (in units of Sv, i.e., 10^6 m^3 s^{-1}) defined as the maximum value of its streamfunction in the North Atlantic Ocean, (b) SST (C), (c) SSS (psu), (d) rate of SST change (C d^{-1}) due to convective adjustment, at a location in the Denmark Strait (30.0W, 65.3N) over the 1,250-year period of the FWN. The initial values of THC, SST, and SSS are enclosed by circles (from MS97).

Because of the sudden onset of the freshwater discharge, the surface of the North Atlantic Ocean is capped by low salinity water with relatively low density. The capping reduces markedly the convective cooling of water, and accordingly, the production of negative buoyancy in the sinking region of the THC. Thus, the THC weakens almost instantaneously, inducing the multi-

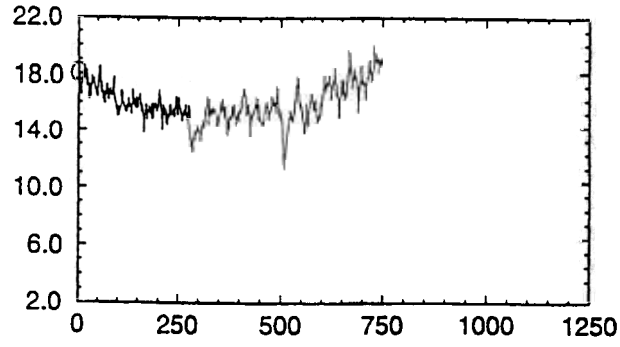

Fig. 11. Time series of the annual mean intensity of the THC (in units of Sv, i.e., 10^6 m^3 s^{-1}) obtained from the FWS. The intensity is defined as the maximum value of its streamfunction in North Atlantic Ocean (from MS97).

decadal oscillation which involves the multidecadal fluctuations of not only the intensity of the THC but also SSS and SST. The fluctuation in the density of near-surface water thus generated causes the corresponding variation in convective activity, which mixes the cold and fresh surface water with warmer and more saline subsurface water. The temporal variation in the intensity of convective activity (Fig. 10d), in turn, enhances the variability of both SST and SSS.

The reduction of SST during the period of freshwater discharge and its increase after the termination of the discharge are much more gradual than the abrupt reduction and increase of surface air temperature which occurred at the beginning and end of the Younger Dryas period, respectively. However, the rapid changes of SST generated by the multidecadal fluctuation of the THC are almost as abrupt as the rise and fall of SST associated with the Y-D.

4.2. FWS

In this subsection, we evaluate the impact of the subtropical discharge of freshwater upon the coupled model

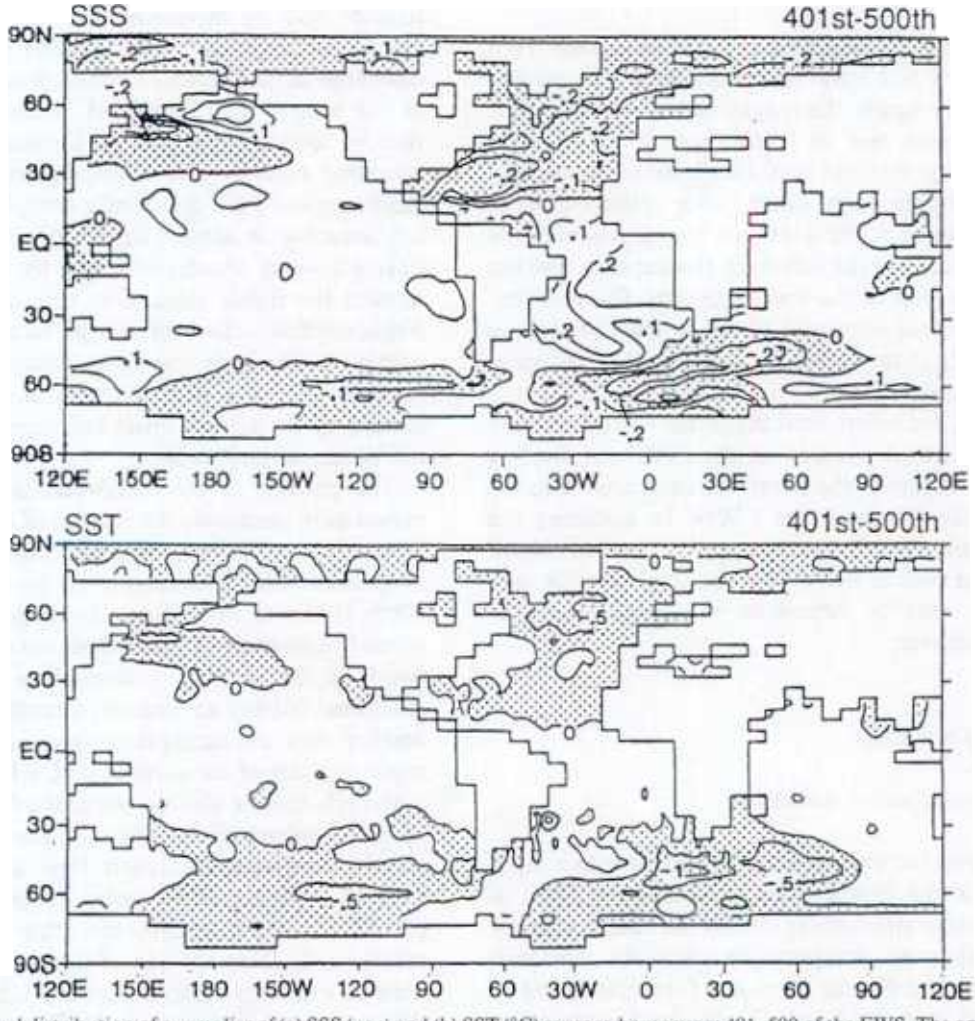

Fig. 12. Geographical distribution of anomalies of (a) SSS (psu) and (b) SST (°C) averaged over years 401–500 of the FWS. The anomalies are defined as the difference between the FWS and control experiment (from MS97).

in comparison to the high-latitude discharge experiment (i.e., FWN) described in the preceding subsection. As noted earlier, the magnitude and duration of the subtropical freshwater discharge are identical to those of the high-latitude discharge for easier comparison. However, the negative SSS anomalies in the North Atlantic Ocean are much smaller in the FWS than in the FWN during the course of the experiments (compare Fig. 12a with Fig. 3). Thus, the total reduction of the THC intensity during the period of the freshwater discharge is smaller in the FWS than in the FWN by a factor of ~ 5 (see Fig. 11 and 10a). As a matter of fact, the THC in the FWS stops weakening a few hundred years before the termination of the freshwater discharge in the 500th year of the experiment (Fig. 11). In sharp contrast to the FWN, in which the THC weakens markedly and negative SSS anomalies are enhanced in the northern North Atlantic due to the reduction in the northward advection of relatively saline surface water by the THC , the freshwater-induced, subtropical SSS anomalies in the FWS are reduced by oceanic advection and remain small in the entire North Atlantic Ocean.

The horizontal distributions of SST anomalies from the FWN and FWS may be compared by inspecting Figs. 6 and 12b. Again, the magnitude of negative SST anomalies is much less in FWS than in FWN. It is notable, however, that the two distributions of the SST anomalies resemble each other, with relatively large negative anomalies in the northern North Atlantic, the Circumpolar Ocean of the Southern Hemisphere, and the northwestern region of the Pacific Ocean. The distributions of the thermal responses of the coupled model are similar, not only at the surface but also in the subsurface layers of the model ocean.

In summary, the subtropical discharge of freshwater is much less effective in weakening the THC and altering the thermal structure of the oceans as compared with the high-latitude discharge in the FWN. In assessing the impact of a meltwater discharge upon a so-called abrupt climate change such as the Y-D event, it is therefore very important to reliably determine the location of the meltwater discharge.

5. Concluding remarks

5.1. Surface temperature variation

In response to the discharge of freshwater into a high-latitude belt of the North Atlantic Ocean, the THC of a coupled ocean–atmosphere model weakens, thereby reducing surface air temperature over the northern North Atlantic, the Nordic Seas, and Greenland, and to a lesser degree, over the Arctic Ocean, the Scandinavian peninsula, Labrador, and the Circumpolar Ocean of the Southern Hemisphere. Upon termination of the freshwater discharge at the 500th year of the experiment, the THC begins to reintensify, gaining its original intensity in a few hundred years. In contrast to the Pacific sector of the Circumpolar Ocean where surface air temperature does not begin to increase until the 800–900th year, the climate of the northern North Atlantic and surrounding regions starts recovering as soon as the freshwater discharge is terminated at the 500th year of the experiment.

The sudden onset and termination of the massive discharge of freshwater also induces a multidecadal fluctuation in the intensities of the THC and convective activity which generate large synchronous fluctuations of both SST and SSS in the northern North Atlantic and surrounding Oceans. Such oscillation yields almost abrupt changes of climate which involves rapid rise and fall of surface temperature in a few decades. The rapid change of SST, thus generated, is almost as abrupt as the changes of SST at the beginning and the end of the Y-D period. In an earlier numerical experiment, Manabe and Stouffer (1995) generated an even more abrupt falls and rises of SST by increasing the rate of freshwater discharge. In response to the sudden onset of a massive discharge of freshwater into the northern North Atlantic at the rate of 1 Sv, the THC weakened very rapidly, thereby lowering the SST in Denmark Strait and surrounding regions. Upon suspension of the freshwater discharge, the THC exhibited a complex transient behavior, inducing an almost abrupt fall, rise and fall of SST during several decades followed by a gradual recovery toward the initial state. One can speculate that high-frequency fluctuations of isotopic temperature, which are evident in the high-resolution records from Greenland ice cores (e.g., Fig. 4 of Jouzel et al., 1995) may also be caused by the abrupt onset and termination of massive discharges of meltwater.

The pattern of the freshwater-induced cooling obtained here resembles the pattern of the Y-D cooling, as inferred from the comprehensive analysis of ice cores and deep-sea and lake sediments (see, for example, Broecker, 1995). However, the region of cooling in the North Atlantic and surrounding regions does not extend as far southward as that of the Y-D cooling. Furthermore, the simulated cooling at Summit, Greenland, appears to be smaller than the actual cooling estimated from the isotopic analysis of ice cores (e.g., GRIP Members, 1993). Although cooling also occurs in the Circumpolar Ocean of the Southern Hemisphere, it does not extend sufficiently northward to reach New Zealand, where the Franz Joseph glacier advanced during the Y-D (Denton and Hendy, 1994). We speculate that these discrepancies result partly from the use of the simulated modern climate as a control rather than the much colder climate of the last deglaciation period. The extensive coverage of sea ice during the cold deglaciation period could not

only have extended the regions of cooling toward lower latitudes but could also have increased its magnitude. Therefore, it is desirable to conduct additional freshwater experiments using the simulated climate of the last deglaciation period as a control.

Improving the earlier results of Guilderson et al. (1994), Guilderson (1996) obtained the high-resolution time series of SST based upon the Sr/Ca thermometry of Barbados corals. His time series indicates that the surface temperature of the western tropical Atlantic fell rapidly during the late Bölling period (between 15 and 13.8 kyr BP), when a massive discharge of freshwater (identified as mwp-IA by Fairbanks, 1989) took place. Guilderson et al. found that the tropical surface temperature rises rapidly upon termination of the mwp-IA (i.e., around 13.7 kyr BP). It is notable, however, that the Sr/Ca temperature in the tropical Atlantic did not change substantially at the beginning of the Y-D (i.e., around 13 kyr BP), despite the abrupt drop of surface temperature in high Atlantic latitudes.

These findings are not inconsistent with the results of the present FWN experiment in which SST in tropical latitudes hardly changes (Fig. 10) despite the large meltwater-induced change in the intensity of the THC. On the other hand, the rapid fall of Sr/Ca temperature in the western tropical Atlantic during the late Bölling (between 15 and 13.8 kyr BP) could result from the cooling of the mixed-layer ocean caused by a massive discharge of cold freshwater into the Gulf of Mexico, as suggested by Guilderson (1996).

One should note, however, that Thompson et al. (1995) found evidence of the Y-D cooling in the tropical atmosphere based upon the isotopic analysis of two ice cores obtained from the col of Huascarán (9° 06′ S, 77° 36′ W). In view of the fact that simulated SST increases very slightly from middle-to-low latitudes in response to the freshwater discharge, the tropical cooling during the Y-D may not be caused by the weakening of the THC which was induced by the discharge of freshwater. Instead, it may have been caused by other factors such as growth of continental ice sheets with high albedo and the reduction in the atmospheric concentration of methane (Chappellaz et al., 1993).

5.2. *Meltwater pulses*

Two numerical experiments are conducted in the present study. In the first experiment discussed above (FWN), freshwater is discharged into the high North Atlantic latitudes which include the sinking regions of the THC, whereas freshwater is applied to a region of the subtropical Atlantic in the second experiment (FWS). In the FWN, the THC weakens because of the capping of the sinking regions by relatively fresh, low-density surface water. On the other hand, the negative SSS anomaly over the sinking regions is much smaller and much less effective for weakening the THC in the FWS in which freshwater is discharged to the subtropical Atlantic.

The contrast between the results from these two experiments encourages the speculation that, at the beginning of the Y-D period, a large amount of meltwater was discharged into high rather than low North Atlantic latitudes. As noted in the introduction of this paper, Broecker et al. (1988) speculated that meltwater was diverted from the Mississippi to the St. Lawrence Rivers around that time. However, de Vernal et al. (1996) did not find convincing evidence for such diversion. One could therefore speculate that the northward transport of heat by the active THC during the warm period of Alleröd could have induced the accelerated melting of the Fennoscandian Ice sheets. The increase in the runoff of meltwater in turn slowed down the THC in the Atlantic Ocean. This speculation appears to be consistent with the high-resolution records of oxygen isotopes and the summer SSTs determined from the taxonomic composition of diatoms in a Norwegian Sea Core (Karpuz and Jansen, 1992). Despite the rapid drop of the diatom temperature from the Alleröd to Y-D, the oxygen isotope anomaly (adjusted for global ice volume) decreases steadily with time, suggesting the possible discharge of meltwater from the Fennoscandian Ice sheets at the onset of the cold Y-D period.

As noted already, the coral records of sea level indicate that the so called meltiwater pube 1A (mwp-1A) ended several hundred years before the onset of the Y-D (Fairbanks, 1989; Bard et al., 1996). Keigwin et al. (1991) and Fairbanks et al. (1992) traced a possible origin of this meltwater discharge back to the Gulf of Mexico. The comparison between the FWN and FWS experiments suggests that the subtropical discharge of meltwater such as the mwp-1A may be much less effective than the high-latitude discharge in weakening the THC. However, the massive amount of freshwater involved in the mwp-1A could be sufficient to weaken the THC significantly and induce the cooling of the past Bölling period (between 15 and 13.8 kyr BP).

As discussed in Section 4.1, the North Atlantic discharge of freshwater affects the sea surface temperature in the Circumpolar Ocean of the Southern Hemisphere. However, the isotopic analysis of Antarctic ice cores reveals that a period of cooling, called Antarctic Cold Reversal (ACR), occurred at least 1000 years before the Y-D (Jouzel et al., 1995). Therefore, it is not very likely that the abrupt cooling of North Atlantic at the beginning of the Y-D is associated with the ACR. Instead, one can speculate that the rapid cooling of North Atlantic during the post-Bölling period could be related to the ACR. Recently, Steig et al. (1998) identified the abrupt warming at the end of the Y-D in an ice core from the Taylor Dome located in the western Ross Sea Section of Antarctica. It appears that the results of

ice core analysis described above do not contradict with the results from the numerical experiments conducted here.

5.3. Two stable equilibria

Manabe and Stouffer (1988) found that their coupled ocean–atmosphere model has at least two stable equilibria with active and inactive modes of the THC in the North Atlantic Ocean. The active mode resembles the current state of the THC with a sinking region in the northern North Atlantic, whereas the inactive mode is characterized by a weak, reverse cell of the THC with sinking motion in the Circumpolar Ocean of the Southern Hemisphere and no ventilation of subsurface water in the North Atlantic Ocean. They suggested that an oceanic state similar to the inactive mode prevailed during the period of the Y-D. Paleoceanographic evidence, however, does not necessarily support this suggestion. Although the deep-sea cores from the North Atlantic Ocean indicate markedly reduced deep-water formation (Boyle and Keigwin, 1987; Keigwin and Lehman, 1994), the distribution of benthic $\delta^{13}C$ estimated by Sarnthein et al. (1994) suggests that an upper deep-water production of significant magnitude did occur during the Y-D. Paleoceanographic evidence (Boyle and Keigwin, 1987; Duplessy et al., 1988) indicates that the Atlantic Ocean of the Last Glacial Maximum (LGM) is also significantly different from the inactive mode of the THC obtained by Manabe and Stouffer (1988). It is characterized by not only the absence of lower deep -water production and enhanced northward penetration of the Antarctic bottom water, but also significant ventilation of the upper deep-water. Thus, it is likely that the North Atlantic Ocean of the Y-D or the LGM are more similar to the transient state of the weakened and shallow THC (obtained from the present experiment) than the equilibrium state of the inactive THC obtained earlier by Manabe and Stouffer (1988).

The coupled model used here also possesses the two stable equilibria which are similar to those obtained by Manabe and Stouffer (1988). Once it is induced, the state of the inactive mode of the reverse THC is stable and remains unchanged over the period of at least several thousand years. Despite the heating due to the vertical thermal diffusion, the temperature of the bottom water does not increase because of the cooling due to the formation of the Antarctic bottom water. Thus the stratification of the deeper layer of the model ocean remains unchanged, preventing the re-activation of the THC.

These results differ from what Schiller et al. (1997) obtained using a coupled ocean–atmosphere model developed at the Max-Planck-Institute (MPI) in Hamburg, Germany. In response to the input of a massive amount of freshwater, the THC of the MPI model collapsed into the inactive, mode of the reverse THC, which is qualitatively similar to the inactive mode obtained by Manabe and Stouffer (1988). However, upon termination of the freshwater discharge, the THC intensified rapidly, eventually regaining its original intensity, in sharp contrast to the behavior of the inactive, reverse mode obtained by Manabe and Stouffer (1988). The difference in behavior between the GFDL and MPI models identified above may be attributable to the difference in the magnitude of diapycnal diffusion in them. Specifically, the oceanic component of the coupled model used by Schiller et al. (1997) employs the first-order, upstream finite difference technique for the computation of advection and, therefore, has relatively large implicit, computational diffusion (see, for example, Wurtele, 1961; and Molenkamp, 1968). It is likely that the large diapycnal diffusion of potential temperature and salinity facilitates the movement of water across isopycnal surfaces, resulting in the reintensification of the THC and the resumption of North Atlantic deep-water formation which occurred after the termination of massive freshwater discharge in the numerical experiment conducted by Schiller et al., 1997.

In order to evaluate this speculation, we recently conducted a similar freshwater experiment using a modified version of the GFDL coupled model in which the coefficient of vertical subgrid scale diffusion in the upper 2 km layer of oceans is several times larger than in the standard version (Manabe and Stouffer, 1999). Although the reverse THC was produced in this version of the coupled model in response to the massive discharge of freshwater, it began to transform rapidly back to the original, direct THC as soon as the freshwater discharge was terminated, in qualitative conformity with the behavior of the MPI model.

Our results clearly indicate that the inactive mode of the reverse THC is not a stable state in a coupled model which has a large diapycnal diffusion coefficient for oceanic subgrid scale mixing. Measurement of the invasion of anthropogenic tracers, such as bomb tritium and ^3He, have indicated that the coefficient of vertical diapicnal mixing in the ocean thermocline of the subtropical North Atlantic is less than 0.1 $cm^2\ s^{-1}$ (Jenkins, 1980) or about 0.2 $cm^2\ s^{-1}$ (Rooth and Östlund, 1972). Based upon the results from a recent field experiment (Ledwell et al., 1994), the most likely value of the effective vertical diffusion coefficient in the ocean thermocline is 0.1–0.2 $cm^2\ s^{-1}$. Even the standard version of the GFDL coupled model, which has the inactive, reverse THC, has a larger vertical diffusion coefficient than these values. Therefore, it is likely that the mode of the reverse THC is also stable in the real Atlantic Ocean in which vertical diffusion appears to be small.

When a coupled model with sufficiently low vertical diffusion coefficient enters the stable state of the reverse THC, it does not get out of it easily (see also Rahmstorf,

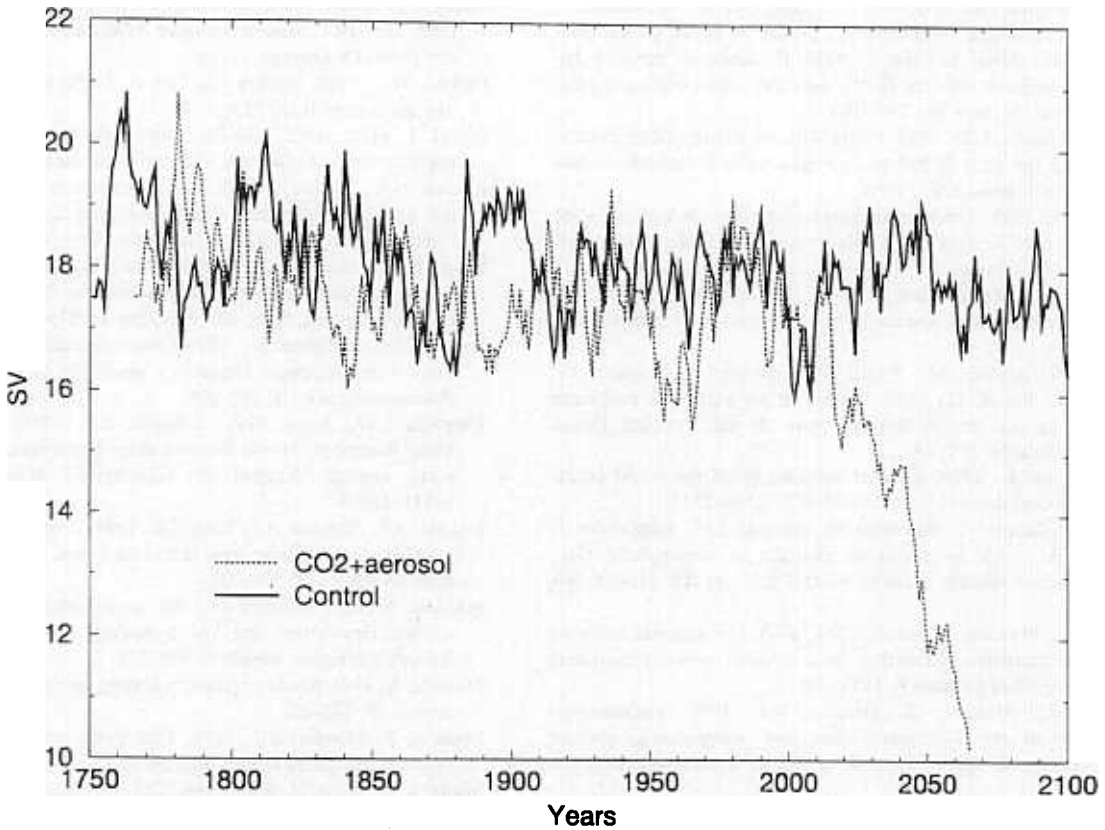

Fig. 13. Temporal variation of the intensity of the thermohaline circulation from the control (solid line) and the thermally forced experiments (dotted line) which were conducted by Haywood *et al.* (1997) using the coupled model. Here the intensity is defined as the maximum value of the stream function representing the meridional overturning circulation in the North Atlantic Ocean (from Manabe (1998)). Units are in Sverdrups (1 Sv = $10^6 m^3 s^{-1}$).

1995). This is another important reason why we believe that the cold state of Y-D was not a stable state of no deep-water formation in the North Atlantic Ocean. Instead, it is a temporarily weakened state of the THC. As noted already, the paleoceanographic signature of deep-water formation is consistent with this assertion.

5.4. *Future change*

The results obtained here could be relevant to the future change of climate. For example, a recent studies by Haywood et al. (1997) and Manabe (1998) reveal that, in response to the time-dependent, radiative forcing by not only greenhouse gases but also anthropogenic sulfate, the THC begins to weaken sometime during the first half of the 21st century (Fig. 13). Associated with the warming of the model atmosphere, the poleward transport of water vapor in the atmosphere increases, resulting in the marked increase in precipitation in high latitudes, and accordingly, the increased freshwater supply to the Arctic and surrounding oceans. Thus, these oceans are covered by near-surface water of low salinity, thereby weakening the THC. Because of the weakening, the northward advection of warm, saline water is reduced, moderating the warming in the North Atlantic and surrounding regions (see also Manabe (1991) for further discussion). The multiple century response of the THC to the doubling and quadrupling of the atmospheric CO_2 concentration was the subject of extensive discussion in the studies of Manabe and Stouffer (1994). The last report of the Intergovernmental Panel on Climate Change (1996) compares the greenhouse gas-induced changes in THC which have been obtained from various coupled ocean–atmosphere models constructed by various groups. In order to detect future change in the intensity of the THC, it is urgent to monitor the structure of water masses in not only the North Atlantic but also the Arctic Ocean and Nordic Seas.

References

Bard, E., Hamelin, B., Arnold, M., Montaggioni, L., Cabioch, G., Faure, G., Rougerie, F., 1996. Deglacial sea-level record from Tahiti corals and the timing of global meltwater discharge. Nature 382, 241–244.

Bond, G., Heinrich, H., Broecker, W., Labeyrie, L., McManus, J., Andrews, J., Huon, S., Jantschik, R., Clasen, S., Simet, C., Tedesco, K., Klas, M., Bonai, G., Ivy, S., 1992. Evidence for massive discharges of icebergs into the North Atlantic Ocean during the last glacial period. Nature 360, 245–249.

Boyle, E.A., Keigwin, L.D., 1987. North Atlantic thermohaline circulation during the past 20,000 years linked to high-latitude surface temperature. Nature 330, 35–40.

Broecker, W.S., 1995. The glacial world according to Wally. Eldigo Press, Lamont-Doherty Earth Observatory, Palisades, New York, 318 pp. + Appendix.

Broecker, W.S., Peteet, D., Rind, D., 1985. Does the ocean-atmosphere system have more than one stable mode of operation?. Nature 315, 21–25.

Broecker, W.S., Andree, M., Wolli, W., Oeschger, H., Bonani, G., Kennett, J., Peteet, D., 1988. A case in support of a meltwater diversion as the trigger for the onset of the Younger Dryas. Paleoceanography 3, 1–19.

Bryan, K., Lewis, L., 1979. A water mass model of the world ocean. Journal of Geophysical Research 84 (C5), 2503–2517.

Chappallaz, J., Blunler, T., Raynaud, D., Barnola, J.M., Schwander, J., Stauffer, B., 1993. Synchronous changes in atmospheric CH_4 and Greenland climate between 40 and 80 K yr BP. Nature 366, 443–445.

Delworth, T.L., Manabe, S., Stouffer, R.J., 1993. Interdecadal variation of the thermohaline circulation in a coupled ocean–atmosphere model. Journal of Climate 6, 1993–2011.

Delworth, T.L., Manabe, S., Stouffer, R.J., 1997. Multidecadal variability in the Greenland Sea and surrounding regions: a coupled model simulation. Geophysical Research Letters 24, 257–260.

de Vernal, A., Hillaire-Marcel, C., Bilodeau, G., 1996. Reduced meltwater outflow from the Lawrentide ice margin during the Younger Dryas. Nature 381, 774–777.

Dixon, K.W., Bullister, J.L., Gamon, R.H., Stouffer, R.J., 1996. Examining a coupled air-sea model using CFCs as oceanic tracers. Geophysical Research Letters 23, 1957–1960.

Duplessy, J.-C., Shackleton, N.J., Fairbanks, R.G., Labeyrie, L., Oppo, D., Kallel, N., 1988. Deep-water source variation during the last climate cycle and their impact on the global deep water circulation. Paleoceanography 3, 343–360.

Fairbanks, R.G., 1989. A 17,000 year glacio-lustatic sea level record: influence of glacial melting rates on the Younger Dryas event and deep-ocean circulation. Nature 342, 637–642.

Fairbanks, R.G., Charles, C.D., Wright, J.D. 1992. Origin of global meltwater pulses. In: Taylor, R.E., et al. (Eds.), Radiocarbon after Four Decades. Springer, Berlin, 473–500.

Gordon, C.T., Stern, W., 1982. A Description of the GFDL Global Spectral Model. Monthly Weather Review 110, 625–644.

GRIP Members, 1993. Climate instability during the last interglacial period recorded in the GRIP ice core. Nature 364, 203–207.

Grootes, P.M., Stulver, M., White, J.W.C., Johnsen, S., Jouzel, 1993. Comparison of oxygen isotope records from the GISP2 and GRIP Greenland ice cores. Nature 366, 552–554.

Guilderson, T.P., 1996. Tropical Atlantic SSTs over the last 20,000 yrs; Implications on the mechanism and synchroneity of climate change. Ph.D. Thesis, Dept. of Earth and Environmental Sciences. Columbia University, New York.

Guilderson, T.P., Fairbanks, R.G., Rubenstone, J.L., 1994. Tropical temperature variations since 20,000 years ago: modulating interhemispheric climate change. Science 263, 663–665.

Haywood, J., Stouffer, R.J., Wetherald, R.T., Manabe, S., Ramaswamy, V., 1997. Transient response of a coupled model to estimated changes in greenhouse gas and sulfate concentrations. Geophysical Research Letters 24, 1335–1338.

Intergovernmental Panel on Climate Change, 1996. Climate change 1995: The IPCC Second Scientific Assessment. Cambridge University Press, Cambridge, 572pp.

Jenkins, W.J., 1980. Tritium and ^3He in the Sargasso Sea. Journal of Marine Research 38, 533–569.

Jouzel, J., et al., 1995. The two-step shape and timing of the last deglaciation in Antarctica. Climate Dynamics 11, 151–161.

Karpuz, N.A., Jansen, E., 1992. A high-resolution diatom record of the last deglaciation from the SE Norwegian Sea: documentation of rapid climatic changes. Paleoceanography 7, 499–520.

Keigwin, L.D., Jones, G.A., 1989. Glacial-Holocene stratigraphy, chronology and paleoceanographic observations on some North Atlantic sediment drift. Deep-Sea Research 36, 845–867.

Keigwin, L.D., Lehman, S.J., 1994. Deep circulation linked to Heinrich event 1 and Younger Dryas in a middepth North Atlantic Core. Paleoceanography 9, 185–194.

Keigwin, L.D., Jones, G.A., Lehman, S.J., 1991. Deglacial meltwater discharge, North Atlantic deep circulation, and abrupt climate change. Journal of Geophysical Research 96 (C9), 16811–16826.

Ledwell, J.R., Watson, A.J., Law, C.S., 1994. Evidence for slow mixing across the pycnocline from an open-ocean tracer-release experiment. Nature 364, 701–703.

Manabe, S., 1969. Climate and the ocean circulation, I. The atmospheric circulation and the hydrology of the earth's surface. Monthly Weather Review 9, 739–774.

Manabe, S., 1998. Study of global warming by GFDL climate models. Ambio 27, 182–186.

Manabe, S., Stouffer, R.J., 1988. Two stable equilibria of a coupled ocean–atmosphere model. Journal of Climate 1, 841–866.

Manabe, S., Stouffer, R.J., 1993. Century-scale effects of increased atmospheric CO_2 on the ocean–atmosphere system. Nature 364, 215–218.

Manabe, S., Stouffer, R.J., 1994. Multiple-century response of a coupled ocean-atmosphere model to an increase of atmospheric carbon dioxide. Journal of Climate 7, 5–23.

Manabe, S., Stouffer, R.J., 1995. Simulation of abrupt climate change induced by freshwater input to the North Atlantic Ocean. Nature 378, 165–167.

Manabe, S., Stouffer, R.J., 1997. Coupled ocean–atmosphere model response to freshwater input: comparison to Younger Dryas event. Paleoceanography 12, 321–336.

Manabe, S., Stouffer, R.J., (1999). Are two modes of thermohaline circulation stable? Tellus, to be published.

Manabe, S., Stouffer, R.J., Spelman, M.J., Bryan, K., 1991. Transient response of a coupled ocean–atmosphere model to gradual changes of atmospheric CO_2 Part I: annual mean response. . Journal of Climate 4, 785–818.

Marotzke, J., 1990. Instability and multiple equilibria of the thermohaline circulation. Ph.D. Thesis, Christian-Albrecht Universität. Kiel, 126.

Molenkamp, C.R., 1968. Accuracy of finite difference methods applied to the advection equation. Journal of Applied Meteorology 7, 160–167.

Peteet, D., 1995. Global Younger Dryas?. Quart. Int. 28, 93–104.

Rahmstorf, S., 1995. Bifurcations of the Atlantic thermohaline arculation in Atomosphere to changes in the hydrologic cycle. Nature 378, 145–149.

Rooth, C.G., Östlund, H.G., 1972. Penetration of tritium into the Atlantic thermocline. Deep Sea Research 19, 481–492.

Sarnthein, M., Winn, K., Jung, S.A., Duplessy, J.-C., Labeyrie, L., Erlenkeuser, H., Gaussen, G., 1994. Changes in east Atlantic deep water circulation over the past 30,000 years: eight times slice reconstruction. Paleoceanography 9, 209–267.

Schiller, A., Mikolajewicz, U., Voss, R., 1997. The stability of the thermohaline circulation in a coupled ocean–atmosphere general circulation model. Climate Dynamics 13, 325–348.

Steig, E.J., Brook, E.J., White, J.W.C., Sucher, C.M., Bender, M.L., Lehman, S.J., Morse, D.L., Waddington, E.D., Clow, G.D., 1998. Synchronous climate change in Antarctica and the Northe Atlantic. Science 282, 92–95.

Thompson, L.G., Moseley-Thompson, E., Davis, M.E., Lin, P.-N., Henderson, K.A., Cole-Dai, J., Bolzan, J.F., Liu, K.-B., 1995. Late glacial stage and Holocene tropical ice core records from Huascarán. Peru. Science 269. 46–50.

Winton, M., 1997. The effect of cold climate upon North Atlantic deep water formation in a simple ocean–atmosphere model. Journal of Climate 10, 39–51.

Wurtele, M.G., 1961. On the problem of truncation error. Tellus 13, 379–391.